

General Disclaimer

One or more of the Following Statements may affect this Document

- This document has been reproduced from the best copy furnished by the organizational source. It is being released in the interest of making available as much information as possible.
- This document may contain data, which exceeds the sheet parameters. It was furnished in this condition by the organizational source and is the best copy available.
- This document may contain tone-on-tone or color graphs, charts and/or pictures, which have been reproduced in black and white.
- This document is paginated as submitted by the original source.
- Portions of this document are not fully legible due to the historical nature of some of the material. However, it is the best reproduction available from the original submission.

NASA CR-73-372

AVAILABLE TO THE PUBLIC

Final Technical Report

Volume 1

Low Energy Proton Effects on
Solar Cell Cover Glass Materials

by Malcolm A. Lillywhite

November 69

Distribution of this report is provided in the interest
of information exchange. Responsibility for the contents
resides in the author or organization that prepared it.

Prepared under Contract No. NAS 2-5083 by
Martin Marietta Corp., Research Department
Denver, Colorado

For

Ames Research Center

National Aeronautics and Space Administration

N70-25005

FACILITY FORM 602 (ACCESSION NUMBER)	(THRU)
24 (PAGES)	
CR-73372 (NASA CR OR TMX OR AD NUMBER)	(CODE) 18 (CATEGORY)

Low Energy Proton Effects on
Solar Cell Cover Glass Materials

Malcolm A. Lillywhite

Martin Marietta Corp., Research Department
Denver, Colorado

National Aeronautics and Space Administration

ABSTRACT

The stability of the spectral transmission in the spectral region .3 to 2.2 μ of Solar cell cover glass materials when exposed to the simulated solar wind proton environment has been evaluated. The test specimens were irradiated with 2 and 3 Kev protons separately and combined with simulated solar electromagnetic radiation. Proton fluxes were nominal 2×10^{11} p/cm² sec where fluences of 5×10^{17} p/cm² were obtained. The material irradiated include 0211 microsheet and 7940 fused silica with and without MgF₂ anti-reflective coatings and were tested at 140°K, 300°K and 400°K. Samples of these materials were irradiated in 1) a "clean" vacuum system, and 2) intentionally contaminated with 704 diffusion pump condensate and then placed in a "clean" vacuum system for irradiation. A model is presented which attempts to explain discrepancies in reported proton damage to MgF₂ and is based on a contaminant film build-up on the MgF₂ surface. No optical damage was observed in the spectral region specified for any material tested under a combination of test conditions. X-ray diffraction characterization showed, however, that the crystallinity of the MgF₂ thin film was altered by irradiation but no optical damage correlation was possible.

Technical Objective

The purpose of this program was to study the effects of exposure to the simulated solar wind environment on the optical stability of solar cell cover glasses which may or may not employ an antireflective coating. Specifically this means to evaluate the effects of 1) simulated solar wind proton energy, flux and fluence 2) sample temperature during irradiation and 3) combined electromagnetic and corpuscular irradiation (synergistic or anti-energetics effects) on the transmission characteristics of cover glass materials in the spectral region .3 to 2.2 μ . The study has concentrated on the evaluation of the vapor deposited magnesium fluoride thin film used as an antireflective coating, although two other materials (substrates) were evaluated. The criteria for evaluation of these materials was primarily irradiation induced changes (damage) in spectral transmission. Since no such damage was observed during this program the technical depth of the analysis and the cross correlation of other methods of materials characterization to the optical damage will be, necessarily, a minimum. However, X-ray diffraction was used on several of the samples before and after irradiation to characterize the nature of the crystal structure or changes in the event any optical damage was observed.

Introduction to The Problems

Recent data indicate that the cover slide materials utilizing an antireflective coating experience a severe transmission loss ($> 40\%$) when irradiated with 2.0 Kev protons to a fluence of $5 \times 10^{17} \text{ p/cm}^2$.* The report containing these data attributes this damage to the magnesium fluoride antireflective coating on the front side of the cover slide material. The limited data available here pointed out the need for a more comprehensive study designed to evaluate these cover slide materials using accurately simulated and controlled space environment conditions and substantiated measurement techniques. The program which this report summarizes was designed to provide this data and to provide the experimental data required for selection of stable antireflective coatings and substrate materials for solar cell cover slides and for prediction of their performance during interplanetary missions.

Employing an antireflective coating on a solar cell surface increases the energy transmitted to the photovoltaic converting surface by approximately 2%. For missions of 1 AU or less, this increase in usable irradiance does not appear to improve the output of the cell unit enough to warrant its use if degradation problems are evident. However, for interplanetary missions of approximately 5.0 AU, the solar total irradiance is 0.04 of a solar constant and, under these conditions, the output of the solar cell unit must be maximized. In this case the use of an antireflective coating, if optically stable significantly improves the output of the conversion device. For this reason the antireflective materials must be evaluated.

The antireflective coating placed on the outer surface of solar cell cover slides reduces the reflecting losses at the cover slide surface. Antireflective coating materials must satisfy several criteria, both optical and mechanical, to effectively reduce reflective losses. The index of refraction of a single coating layer, n , must satisfy

$$n^2 = n_1 n_2$$

where n_1 and n_2 are the refractive indices of the materials on either side of the antireflective coating. For the vacuum/ SiO_2 interface, we have $n_1 = 1$, $n_2 = 1.5$ so that $n = 1.2$. The coating thickness must be approximately $1/4$ wavelength in the optical region and must also satisfy the requirements of high stability, low optical absorption, high resistance to abrasion, and reasonable

*Summary report prepared by D. J. Curtin of a symposium entitled, Solar Cells At Synchronous Altitudes, held at Communications Satellite Corporation, Washington, D.C., March 15, 1968, p 8.

cost. Although a single-layer coating provides ideal anti-reflective properties at only one wavelength, the reflectance rises slowly on either side of the minimum so this single coating can provide good antireflective properties over the range of wavelengths important to solar cell operation.

Technical Discussion

Composition of the antireflective and ultraviolet filter coatings: The initial effort of this program was devoted to the study and characterization of the magnesium fluoride (MgF_2) material as a vacuum deposited thin film, the cover glass structure, and the fabrication technique used to produce the cover slides. This approach was taken primarily because a better understanding of the MgF_2 thin film and substrate was needed. The technique used as the basic characterization tool was X-ray diffraction. With this tool, it was possible to study the crystal structure (or changes in) specifically, the stress levels, stoichiometry and crystal order of the material. This technique looks at crystal planes (surfaces) that are most nearly parallel to the substrate. The results obtained from this phase of the study points out some very peculiar characteristics of these thin films.

A composition and constituency model has been constructed from information about the materials fabrication procedure. This information was obtained from various conversations with Optical Coating Laboratories, Inc., Santa Rosa, California (OCLI) personnel and a visit to this plant. The antireflection coating is vacuum deposited on the substrate material at a substrate temperature of $600^{\circ}K$ utilizing a sample table rotating about an eccentric axis with respect to the MgF_2 source. This technique results in a continuously varying angle of deposition. The MgF_2 crystal material is held in an alumina (Al_2O_3) crucible and radiatively heated to a vaporization state from above with a tungsten filament. This vacuum deposition technique introduces the possibilities of Al_2O_3 and W (tungsten or wolfram) impurities within the thin film crystal structure, as well as the possibility of certain unique local stresses.

When the ultraviolet filter is employed (on the opposite side of the substrate to that of the antireflective coating), thin films of two or more of the following compounds may be used: Cerium Oxide, CeO_2 , Magnesium Fluoride, MgF_2 , Titanium Dioxide, TiO_2 , Silicon Oxide, SiO_x , Si_2O_3 . The MgF_2 , CeO_2 compounds are

used only on microsheet substrates and the TiO_2 and Si_2O_3 compounds are used on the 7940 silica substrates.

The X-ray diffraction technique used to characterize these cover glass materials was accomplished using a Siemen Krystalflex IV Diffractometer with a copper (Cu) target tube which produces a 1.54\AA X-ray beam. The sample is rotated about the center of a table at $\frac{d\theta}{dt}$ and the detector is rotated at $2 \frac{d\theta}{dt}$.

The early work with X-rays was to survey the different cover glass samples to compare the diffraction patterns of samples from different production runs and of different types, as well as to determine what the limits of such a measurement might be. The ultimate use of the tool was to characterize the material before and after irradiation in the simulated space environment to compare induced changes in crystal structure. It was observed early in the investigation that the diffraction pattern of any two cover slides would not be the same. An example of this can be seen in Figures 1 and 2. Both of these samples are from the same production run and it can be seen from the height and width of the peaks that the crystal order is not the same. It is interesting to note that the pattern shown in Figure 3 looks like that pattern shown in Figure 2. and the sample measured in Figure 3 is of a different type and has both antireflective and ultraviolet filter coatings. The difference in the width, or actually the area under the peak, or intensity of the peak, can be influenced here by two factors: 1) the crystallites are very small; or 2) microstresses, many times smaller than the crystallite size ($<100\text{\AA}$) exist. The apparent line shift ($\approx \frac{1}{2}^{\circ}$) that can be observed (periodically) relative to the preferred order of MgF_2 and from one pattern to another can be influenced here by three factors: 1) decrease in unit cell size (which is effectively a variation in density due to non-stoichiometry); 2) macrostresses (compression, tension, and torque in the film; and 3) defects present at a lattice point (e.g., foreign ion replaces Mg ion or F ion). It is felt that since these effects are observed in the cover glass film before irradiation, they are a product of the fabrication procedure, primarily micro and macro stresses. The peak that varies the most is the MgF_2 peak with a Miller Indices of 111 and is observed at $2\theta = 42^{\circ}$ (center peak). This can be seen by comparing all the diffraction patterns. This may be due to acicular or platelet formations, with dimensions on the order of 50\AA thickness and 5000\AA length, that grow during the deposition process. Figures 4 and 5 show the diffraction pattern of two different cover glass samples; Figure 4 differs in substrate thickness and Figure 5 differs in

substrate material. Note the change in the scattering peak of Figure 5, due to the microsheet substrate.

The literature reports that the preferred order of a pure single crystal of MgF_2 should produce its dominant peak at $2\theta = 24^\circ$ with a Miller Indices = 110. The peak is very weak or non-existent in these diffraction patterns. It is obvious from these results that a general characterization of a class or run of cover glasses is not possible. The specific characterization operation must be performed on each sample before it is to be tested. This characterization technique may present a problem if the X-ray irradiation acts as a catalyst or triggering mechanism for damage to the thin film. This phenomenon has been observed on one cover glass sample, and is demonstrated in Figure 6. This diffraction pattern was measured two weeks after the pattern shown in Figure 2 (e.g., same sample). No other irradiation of sample 1 occurred during this time. Apparently, the crystallinity of this film has been destroyed. The resulting crystallite sizes are probably smaller than 20\AA . An attempt to explain or study this further in terms of temporal changes or recovery has not been made; however, it is strongly felt that this may be a stress relief phenomenon. This change in crystallinity did not directly effect the spectral transmission of the coverslide in the region of 0.3 to 2.1 μ . This inadvertent crystal change did not affect the stability of the transmission properties of the film when exposed to the simulated space environment.

Diffraction patterns of the type shown in Figures 8 and 9 caused some concern during the early phase of this investigation. These measurements were made on the only type of samples studied to date that have both antireflective and ultraviolet filter coatings (fused silica substrates). This means that on one side of the cover glass (antireflective) the MgF_2 and on the other (ultraviolet filter) there is TiO_2 and SiO_x and in this case, the substrate is 3 mils thick. Both TiO_2 and MgF_2 are of tetragonal crystal structure. There are two forms of TiO_2 , anatase, which has a face-centered tetragonal geometry, and rutile, which has a body-centered tetragonal geometry. The diffraction patterns of each of these structures will look very much the same. This complicates observations of the crystal changes in the MgF_2 film, particularly when the substrate is thin and the X-ray diffraction pattern can actually record the effects of both films (antireflective and ultraviolet filter). In spite of this rough calculation made from the line shift observed in Figure 8, show that this sample has a unit cell density approximately 1% smaller than normal MgF_2 .

This change may be due to the proton irradiation suffered by this sample.

It is difficult to make any general conclusions based solely on the data presented here; however, the understanding of the nature of these films has been greatly increased. It is apparent that the fabrication process produces cover glass slides which are vastly different in stress characteristics. Because of this and other factors, each slide that was to be analyzed with X-ray diffraction techniques was characterized before and after testing, however no correlation between optical damage due to proton irradiation and change in crystal properties using X-ray diffraction was possible because there were no induced changes in transmission. The bulk of the X-ray diffraction data is contained in the Appendix I, a separate volume.

The X-ray diffraction measurements were made by Gavin Mallett - Chief, X-ray Diffraction Center, Metallurgy Department, University of Denver.

The Space Environment

Two components of the interplanetary space environment that are potentially damaging to the optical properties of anti-reflective coating materials are the solar wind and solar electromagnetic radiation. Since the sun is the source of both of these energetic radiations, their intensity varies inversely as the square of the distance from the sun. The solar wind is an electrically neutral plasma composed of low-energy positive ions with an accompanying flux of ev-range electrons. The ionic component is primarily protons with less than 10% heavier ions, mostly alpha particles. The plasma travels nearly radially outward from the sun with velocities that range from 300 to 500 km/sec for a quiet sun and from 560 to 750 km/sec during active periods. The average proton energy is between 1 and 2 kev and the average flux density at 1 AU is about 1×10^8 protons/cm²-sec.

The total solar electromagnetic irradiance at 1 AU (solar constant) has a value of 140 mw/cm². Over 99% of this total lies in the wavelength range from 0.2 to 4.0 microns -- about 9% in the near ultraviolet (0.2 to 0.4 micron), and the remainder in the infrared. Less than 0.1% of the solar energy lies below 0.2 micron. Radiation in the near ultraviolet is generally considered most damaging because of the high total energy and the relatively high photon energy in this band.

Simulated Space Environment Conditions

The test equipment is designed to simulate the actual space environment conditions as accurately as possible and still perform economically. Where it is necessary to make major compromises in simulated vs. actual parameters the conditions are measured accurately and an attempt is made to correlate this data to actual condition. For example, higher than actual fluxes and total irradiance values were used to reduce test time to reasonable periods. When these anomalies occur they are pointed out in the test matrix.

The vacuum system consists of the exposure chamber, the particle accelerator and mass separator, the mass spectrometer, and the transmission measurement tube. The system is pumped with a 500 liters/second nitrogen capacity Ultek Ion pump. Rough pumping is accomplished with sorption pumps.

The particle accelerator uses a special RF source to generate hydrogen ions that are extracted as a uniform 7.5 - cm-diameter beam. The beam passes into a Bennett tube, an RF-type mass separator,

in which the heavier ions can be removed to provide a pure proton beam. Mass analysis of the unseparate beam used shows 25% H^+ ions protons, 75% H^{++} ions or heavier, (<10% heavier ions). The unseparated beam was used during this program. Following mass separation the protons can be accelerated to an energy variable from 100 to 4000 ev, where the energy distribution curve is estimated to have a 100 volt half height width. Instantaneous proton flux densities in the range from 10^6 to 10^{12} p/cm -sec are available at specimen position. The 7.5-cm beam density varies in spatial uniformity from 20% to 70%. Thermal energy electrons can be injected into the accelerated beam from heated filaments to provide a space-charge neutral beam of solar wind character. This feature was not used however because preliminary tests using Z-93 thermal control coating showed no positive charge build up effects (data contained in appendix). A Faraday cup provides calibration and monitoring of flux density, beam uniformity and collimation, energy spectrum, and beam neutrality in a horizontal plane between sample positions. A mass spectrometer is attached to the system behind the exposure chamber to check, and monitor if desired, purity of the proton beam.

The solar simulator utilizes a high-pressure xenon short-arc lamp. The total irradiance at sample position is adjustable from 0.5 to 7 solar constants ($140 \text{ mw/cm}^2/\text{solar constant}$) by means of a Suprasil quartz lens system. Two 1-inch diameter beams of individually variable intensity pass through Suprasil quartz windows in the test chamber so two of the four samples can be exposed to electro-magnetic radiation. Monitoring of the spectral and total irradiance is provided.

Four individual sample holders are provided in the facility. Provision for heating or cooling and for temperature monitoring is made for each sample holder. A sample transfer assembly removes the samples individually from the sample holders and transfers them to the optical measurement system.

This transmittance measurement unit consists of an evacuated extension that terminates in a cylinder that is capped at the ends by sapphire windows. Test specimens that have been mounted in the sample holders can be transferred (by the standard sample transfer assembly) to the center of the cylinder so the beam must pass through the specimen. A comparison of transmission measurement with and without the specimen in place gives a measurement of the spectral transmittance of the sample. The transmittance measurement is actually a spectral irradiance measurement made of the distribution of irradiance transmitted in each case (e.g. with and without sample in place). The measurement is made with a Cary 14R spectral radiometer.

Test Conditions and Results

The test matrix shown in Table 1 - "Test Matrix for Evaluation of Solar Cell--" presents the specific test conditions for each test and describes each test specimen in detail. The specified samples were irradiated at several different fluxes and temperatures to different fluences. Under no combination of test conditions was any optical damage (change in transmission characteristics) observed. For this reason the bulk of spectral transmittance data is not intimately involved in any conclusions that are drawn in this report and consequently will be contained in a voluminous appendix to this report. Two anomalies exist which are not reflected in the test matrix which must be pointed out. First the sample holder temperature during test #3 was to be maintained as 140°K during the entire test. After discussion with the Technical Monitor midway through the test it was decided to abandon this cryogenic test and continue the test at 300°K. The final transmission measurement of test was also made "in air". Secondly, the two transmission measurements made at the beginning and end of Test #4 were made "in air". The in air measurements were made using a different measurement system to improve the absolute accuracy of the measurement.

Surface Contamination Effects

Test #5 was conducted to investigate the possibility of optical damage resulting from polymerization or other damage that might modify the optical properties of a thin film of 704 diffusion pump oil. Such a film might arrive at the sample surface when tested in a chamber using diffusion pumping. Recent data from the Boeing Company shows this to be true when MgF_2 surfaces are irradiated in a diffusion pumped vacuum system with 4 Kev protons*. There is no facility at MMC which utilizes a diffusion pumping system and can accommodate the low energy proton source. Consequently, the approach taken was to irradiate intentionally contaminated samples in the existing "clean" system. The transmission of the samples was measured, and they were exposed to the vacuum condition in a diffusion pumped system for eighteen hours located at various points near the pumping throat. During this period the baffle was not cooled. At the end of this period, the transmission of the samples was again measured, and they were placed in the "clean" vacuum system for proton irradiation.

* Report given by Roger Gillette of the Boeing Company at the Second Thermophysics Roundtable Meeting on September 7, 1969, in Los Angeles.

All of these measurements were made in air in a Beckman DK2 Spectrophotometer. At a fluence of 1×10^{16} p/cm² the samples were measured again. No damage was observed. There was evidence showing that the film which had been deposited during the eighteen hour exposure had been removed during this test. This was concluded from the shift in interference bands on the O211 microsheet samples with the antireflective coating and ultraviolet filters before and after each exposure. Apparently, to produce an oil film that results in significant optical changes or net damage to the cover slide, a very thin film must be forming during proton irradiation and must react with the radiation and build up a series of damaged layers in this manner. This produces various degrees of optical damage. The Boeing data indicates that this might be the case. Damage under the monolayer formation condition rather than the intentionally deposited thick film (several thousand Angstrom) condition is reasonable if the penetration (or energy) of the proton is considered. In the case of the intentionally deposited thick film, the proton energy is dissipated in the near surface of the oil film, and to produce optical changes, damage must occur to the oil. In the case of simultaneous buildup of the monolayer film, the energy can be dissipated at the oil - MgF₂ interface. This indicates that optical damage due to contamination may require the presence of the MgF₂ thin film, the monolayer of contaminant, and proton irradiation. This naturally occurs at the MgF₂ - oil interface. If this phenomenological model is valid, then much can be determined about the role and nature of various contaminants in the optical modification of particular optical components. It could be determined from knowledge of the availability and temporal distribution of a particular contaminant "a priori" what its role in direct optical modification and in residual radiation induced damage might be. This model is highly tenuous and will vary with different materials and particle species and energy. However, it presents a possible and partially documented explanation of why MgF₂ might show apparent degradation in some simulation facilities and not in others. It also provides foundation for future study in direct and residual contamination effects in the space environment. It is obvious that considerably more study will be necessary before such an approach might become valuable, but it does address itself to one of the major space technology problems of the future.

Conclusion

Proton irradiation in the energy range 2-3 Kev, reaching fluences as high as 5×10^{17} p/cm², of MgF₂ thin film anti-reflective coatings on substrates of O211 microsheet and 7940 fused silica as well as irradiation of the substrates themselves applied in the manner prescribed in this report does not alter the spectral transmission characteristics of said materials in the spectral region 3 to 2.24. The X-ray diffraction characterization does, however, show the crystallinity may be altered under these conditions. No correlation can be made. It is concluded then that optical damage that occurs to similar materials from exposure to these irradiation conditions might be due to surface contamination or diffused surface adsorbed contaminants. This could result from either a faulty production run, from handling, or from residual contaminants in a test chamber or in the space environment. Further investigations might study such contamination problems to determine what impurities might be available in space (and ambient) conditions, and their availability and distribution. This study should identify contaminants which are major contributors to color or other absorption center formations. A superficial model has been presented in an effort to explain existing data and give direction to studies devoted to direct and indirect contamination effects on optical properties.

TEST MATRIX FOR EVALUATION OF SOLAR CELL COVER GLASS MATERIALS IN THE SIMULATED SPACE ENVIRONMENT

NOMENCLATURE			DESCRIPTION OF TEST SPECIMENS									TEST CONDITIONS						
TEST NUMBER	SPECIMEN POSITION	SPECIMEN NUMBER	MATERIAL TYPE	SIZE-LENGTH-WIDTH (cm)	SIZE-THICKNESS (mm)	ANTI-REFLECTIVE COATING (A/R)	ULTRAVIOLET FILTER (UV/F)	SIDE IRRADIATED	PRE-X-RAY DIFFRACTION CHARACTERIZATION	POST-X-RAY DIFFRACTION CHARACTERIZATION	CHARGED PARTICLE FLUX (p/cm ² sec)	SPECIMEN HOLDER TEMPERATURE (°K)	BEAM ENERGY (VOLTS)	ELECTROMAGNETIC RADIATION (W/cm ²)	FLUENCE-TRANSMISSION MEASUREMENT 1	FLUENCE-TRANSMISSION MEASUREMENT 2	FLUENCE-TRANSMISSION MEASUREMENT 3	FLUENCE-TRANSMISSION MEASUREMENT FINAL
1	1	T1S1A	7940 Silica	2x2	3	X	X	A/R	X	X	2.10 ¹¹	20°C	2070	840	0	2.10 ¹⁶	6.10 ¹⁶	2.10 ¹⁷
	2	T1S2A	7940 Silica	2x2	3	X	X	A/R	-	-	2.10 ¹¹	20°C	2070	-	0	2.10 ¹⁶	6.16 ¹⁶	2.10 ¹⁷
	3	T1S3A TOP	7940 Silica	1x2	12	X	-	A/R	X	X	2.10 ¹¹	20°C	2070	-	0	2.10 ¹⁶	6.10 ¹⁶	2.10 ¹⁷
		BOT-T1S3B TOM	7940 Silica	1x2	12	X	-	A/R	-	-	2.10 ¹¹	20°C	2070	-	0	2.10 ¹⁶	6.10 ¹⁶	2.10 ¹⁷
	4	T1S4A TOP	7940 Silica	1x2	12	X	-	A/R	X	X	2.10 ¹¹	20°C	2070	-	0	2.10 ¹⁶	6.10 ¹⁶	2.10 ¹⁷
		BOT-T1S4B TOM	7940 Silica	1x2	12	X	-	A/R	-	-	2.10 ¹¹	20°C	2070	-	0	2.10 ¹⁶	6.10 ¹⁶	2.10 ¹⁷
2	1	T2S1A TOP	7940 Silica	1x2	20	X	-	A/R	-	-	2.10 ¹¹	401	2050	-	0	1.10 ¹⁶	6.10 ¹⁶	1.10 ¹⁷
		BOT-T2S1B TOM	7940 Silica	1x2	20	X	-	A/R	-	-	2.10 ¹¹	401	2050	-	0	1.10 ¹⁶	6.10 ¹⁶	1.10 ¹⁷
	2	T2S2A TOP	7940 Silica	1x2	12	X	-	A/R	X	X	2.10 ¹¹	375	2050	-	0	1.10 ¹⁶	6.10 ¹⁶	1.10 ¹⁷
		BOT-T2S2B TOM	7940 Silica	1x2	12	X	-	A/R	X	X	2.10 ¹¹	375	2050	-	0	1.10 ¹⁶	6.10 ¹⁶	1.10 ¹⁷
	3	T2S3A TOP	0211 Micro	1x2	6	X	-		X	X	2.10 ¹¹	390	2050	840	0	1.10 ¹⁶	6.10 ¹⁶	1.10 ¹⁷
		BOT-T2S3B TOM	0211 Micro	1x2	6	X	-	A/R	-	-	2.10 ¹¹	390	2050	840	0	1.10 ¹⁶	6.10 ¹⁶	1.10 ¹⁷
	4	T2S4A TOP	0211 Micro	1x2	6	X	-	A/R	X	X	2.10 ¹¹	383	2050	-	0	1.10 ¹⁶	6.10 ¹⁶	1.10 ¹⁷
		BOT-T2S4B TOM	0211 Micro	1x2	6	X	-	A/R	-	-	2.10 ¹¹	383	2050	-	0	1.10 ¹⁶	6.10 ¹⁶	1.10 ¹⁷

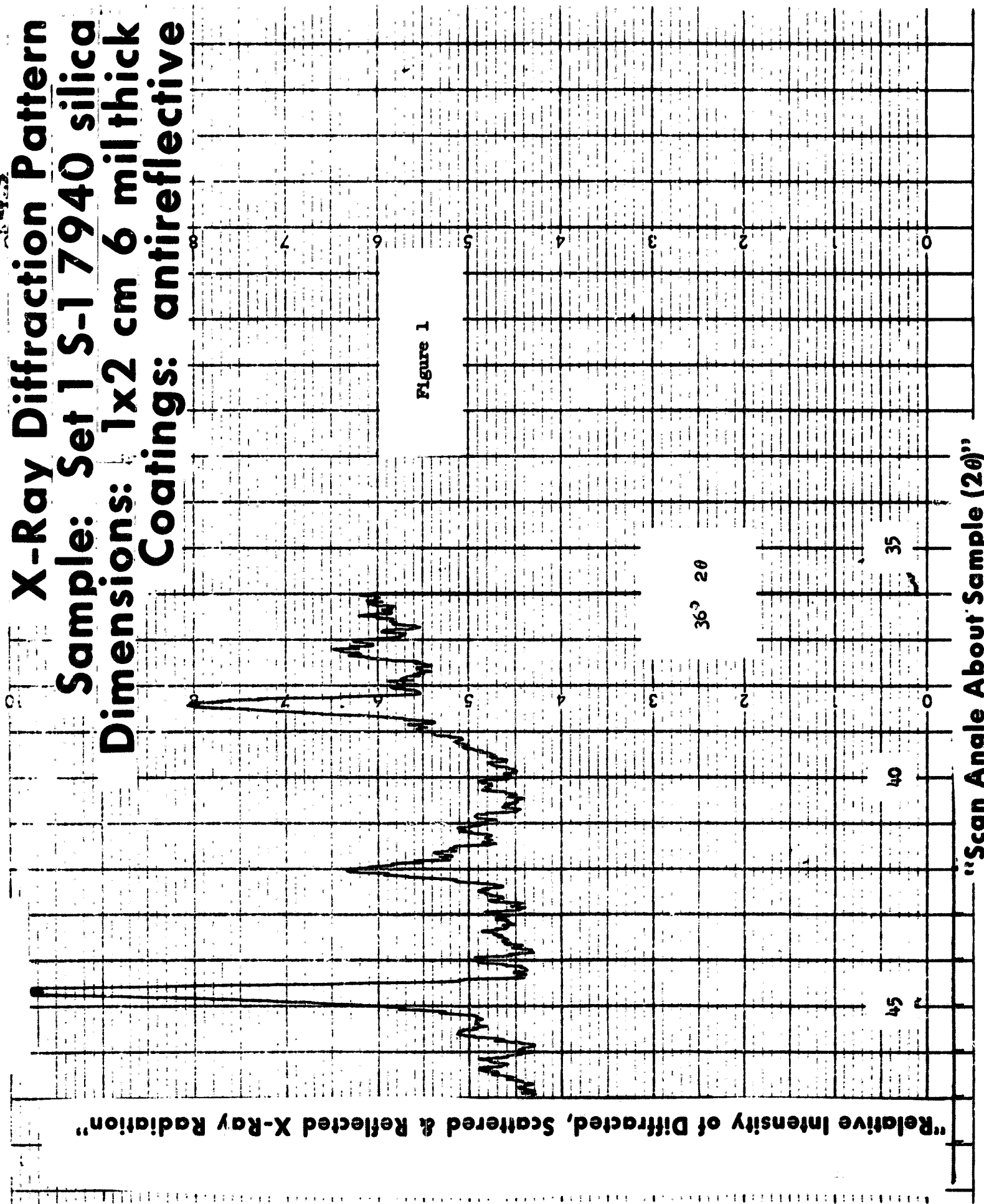
TEST MATRIX FOR EVALUATION OF SOLAR CELL COVER GLASS MATERIALS IN THE SIMULATED SPACE ENVIRONMENT.

NOMENCLATURE				DESCRIPTION OF TEST SPECIMENTS											TEST CONDITIONS						
TEST NUMBER	SPECIMEN POSITION	SPECIMEN NUMBER	MATERIAL TYPE	SIZE LENGTH	WIDTH (cm)	SIZE THICKNESS (cm)	ANTI REFLECTIVE COATING (A/B)	ULTRAVIOLET FILTER (UV/F)	SIDE IRRADIATED	PRE XRAY DIFFRACTION	POST XRAY DIFFRACTION	CHARACTERIZATION	CHARGED PARTICLE	FLUX (p/cm ² sec)	SPECIMEN HOLDER TEMPERATURE (°K)	BEAM ENERGY (VOLTS)	ELECTROMAGNETIC RADIATION (mJ/cm ²)	FLUENCE-TRANSMISSION MEASUREMENT 1	FLUENCE-TRANSMISSION MEASUREMENT 2	FLUENCE-TRANSMISSION MEASUREMENT 3	FLUENCE-TRANSMISSION FINAL MEASUREMENT
3	1	T3S1A	0211 Micro	1X2	6	X	-	A/R	-	X	X	X	2.10 ¹¹	140 & 300	2000	0	2.10 ¹⁶	6.5.10 ¹⁶	1.2.10 ¹⁷		
	BOT-TOM	T3S1B	0211 Micro	1X2	6	X	-	A/R	-	-	-	-	2.10 ¹¹	140 & 300	2000	0	2.10 ¹⁶	6.5.10 ¹⁶	1.2.10 ¹⁷		
	2	T3S2A	0211 Micro	1X2	6	X	X	A/R	X	X	X	X	2.10 ¹¹	140 & 300	2000	0	2.10 ¹⁶	6.5.10 ¹⁶	1.2.10 ¹⁷		
	BOT-TOM	T3S2B	0211 Micro	1X2	6	X	X	A/R	-	-	-	-	2.10 ¹¹	140 & 300	2000	0	2.10 ¹⁶	6.5.10 ¹⁶	1.2.10 ¹⁷		
	3	T3S3A	7940 Silica	1X2	20	X	-	A/R	X	X	X	X	2.10 ¹¹	140 & 300	2000	840	2.10 ¹⁶	6.5.10 ¹⁶	1.2.10 ¹⁷		
	BOT-TOM	T3S3B	7940 Silica	1X2	6	X	-	A/R	-	-	-	-	2.10 ¹¹	140 & 300	2000	840	2.10 ¹⁶	6.5.10 ¹⁶	1.2.10 ¹⁷		
	4	T3S4A	7940 Silica	1X2	20	X	-	A/R	X	X	X	X	2.10 ¹¹	140 & 300	2000	0	2.10 ¹⁶	6.5.10 ¹⁶	1.2.10 ¹⁷		
	BOT-TOM	T3S4B	7940 Silica	1X2	20	X	-	A/R	-	-	-	-	2.10 ¹¹	140 & 300	2000	0	2.10 ¹⁶	6.5.10 ¹⁶	1.2.10 ¹⁷		
4	1	T4S1A	0211 Micro	1X2	6	X	-	Back	-	-	-	-	4.10 ¹¹	300	3000	0	-	-	-	5.10 ¹⁷	
	BOT-TOM	T4S1B	0211 Micro	1X2	6	X	-	A/R	-	-	-	-	4.10 ¹¹	300	3000	0	-	-	-	5.10 ¹⁷	
	2	T4S2A	7940 Silica	1X2	20	-	-	-	-	-	-	-	4.10 ¹¹	300	3000	0	-	-	-	5.10 ¹⁷	
	BOT-TOM	T4S2B	7940 Silica	1X2	20	X	-	A/R	-	-	-	-	4.10 ¹¹	300	3000	0	-	-	-	5.10 ¹⁷	
	3	T4S3A	7940 Silica	1X2	20	X	-	Back	-	-	-	-	4.10 ¹¹	300	3000	0	-	-	-	5.10 ¹⁷	
	BOT-TOM	T4S3B	7940 Silica	1X2	20	X	-	A/R	-	-	-	-	4.10 ¹¹	300	3000	0	-	-	-	5.10 ¹⁷	

TEST MATRIX FOR EVALUATION OF SOLAR CELL COVER GLASS MATERIALS IN THE SIMULATED SPACE ENVIRONMENT

TEST NUMBER	NOMENCLATURE			DESCRIPTION OF TEST SPECIMENTS										TEST CONDITIONS					
	SPECIMEN POSITION	SPECIMEN NUMBER	MATERIAL TYPE	SIZE-LENGTH-WIDTH (cm)	SIZE-THICKNESS (mm)	ANTI-REFLECTIVE COATING (A/R)	ULTRAVIOLET FILTER (UV/E)	SIDE IRRADIATED	PRE XRAY DIFFRACTION CHARACTERIZATION	POST XRAY DIFFRACTION CHARACTERIZATION	CHARGED PARTICLE	FLUX (p/cm ² ·sec)	SPECIMEN HOLDER TEMPERATURE (°K)	BEAM ENERGY (VOLTS)	ELECTROMAGNETIC RADIATION (GW/cm ²)	FLUENCE-TRANSMISSION MEASUREMENT 1	FLUENCE-TRANSMISSION MEASUREMENT 2	FLUENCE-TRANSMISSION MEASUREMENT 3	FLUENCE-TRANSMISSION MEASUREMENT FINAL
4	4 TOP	T4S4A 0211 Micro	0211 Micro	1X2	6	-	-	-	-	4.10 ¹¹	300	3000	-	-	-	-	-	5.10 ¹⁷	
	BOT-T4S4B TOM	0211 Micro	0211 Micro	1X2	6	X	-	A/R	-	4.10 ¹¹	300	3000	-	-	-	-	-	5.10 ¹⁷	
5	1 TOP	T5S1A Silica	7940 Silica	1X2	12	X	-	A/R	-	4.10 ¹¹	300	3000	-	-	-	-	-	1.10 ¹⁶	
	1 BOT	T5S1B Silica	7940 Silica	1X2	12	-	-	-	-	4.10 ¹¹	300	3000	-	-	-	-	-	1.10 ¹⁶	
	2 TOP	T5S2A Micro	0211 Micro	1X2	6	X	-	A/R	-	4.10 ¹¹	300	3000	-	-	-	-	-	1.10 ¹⁶	
	2 BOT	T5S2B Micro	0211 Micro	1X2	6	-	-	-	-	4.10 ¹¹	300	3000	-	-	-	-	-	1.10 ¹⁶	
	3 TOP	T5S3A Micro	0211 Micro	1X2	6	X	X	A/R	-	4.10 ¹¹	300	3000	-	-	-	-	-	1.10 ¹⁶	
	3 BOT	T5S3B Micro	0211 Micro	1X2	6	X	X	A/R	-	4.10 ¹¹	300	3000	-	-	-	-	-	1.10 ¹⁶	
	4 TOP	T5S4A Micro	0211 Micro	1X2	6	X	-	A/R	-	4.10 ¹¹	300	3000	-	-	-	-	-	1.10 ¹⁶	
	4 BOT	T5S4B Micro	0211 Micro	1X2	6	-	-	-	-	4.10 ¹¹	300	3000	-	-	-	-	-	1.10 ¹⁶	

**X-Ray Diffraction Pattern
Sample: Set 1 S-1 7940 silica
Dimensions: 1x2 cm 6 mil thick
Coatings: antireflective**



X-Ray Diffraction Pattern

Sample: Set 1 S-1 7940 silica

Dimensions:

1x2 cm 6 mil thick

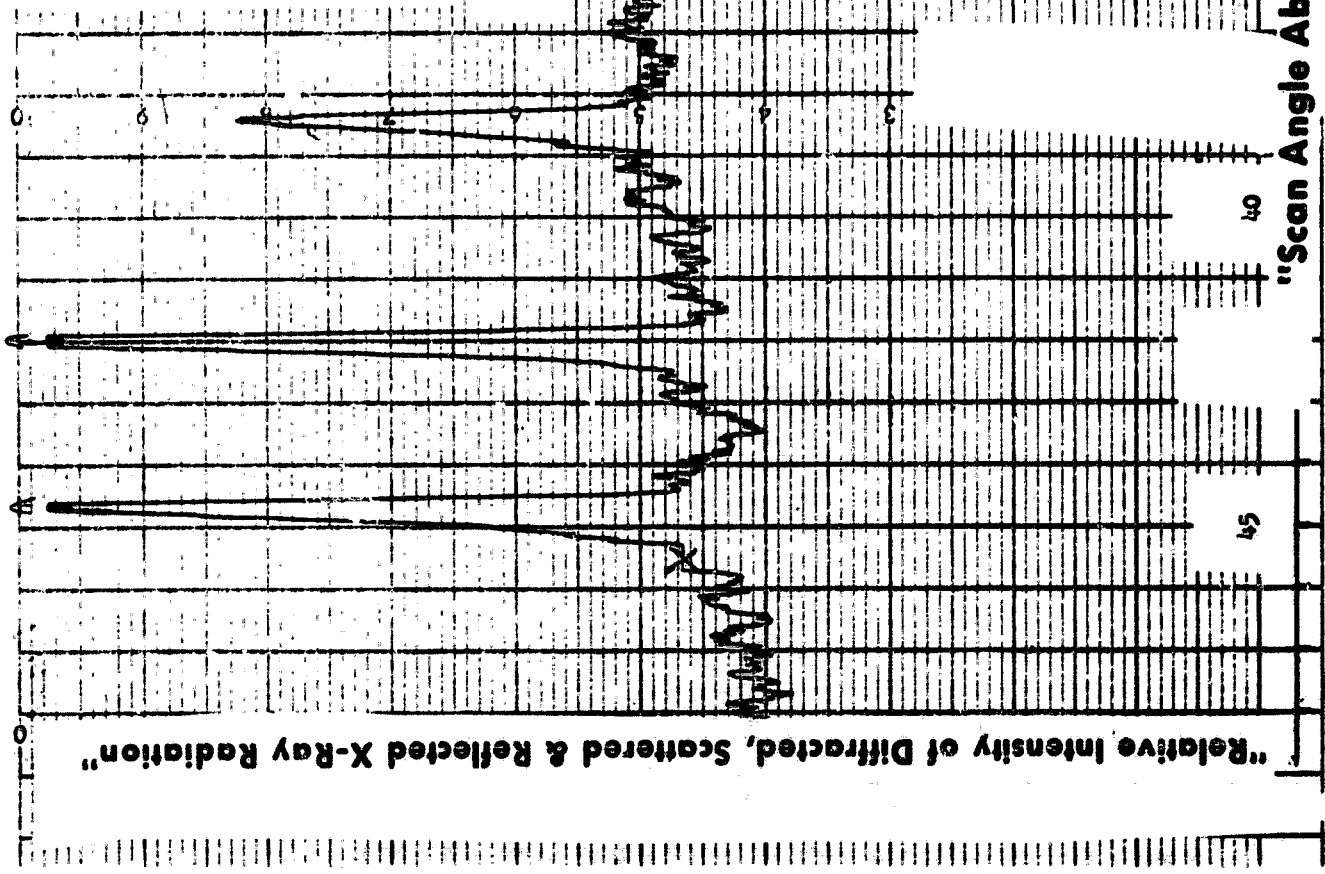
Coating: antireflective
plus ultraviolet filter

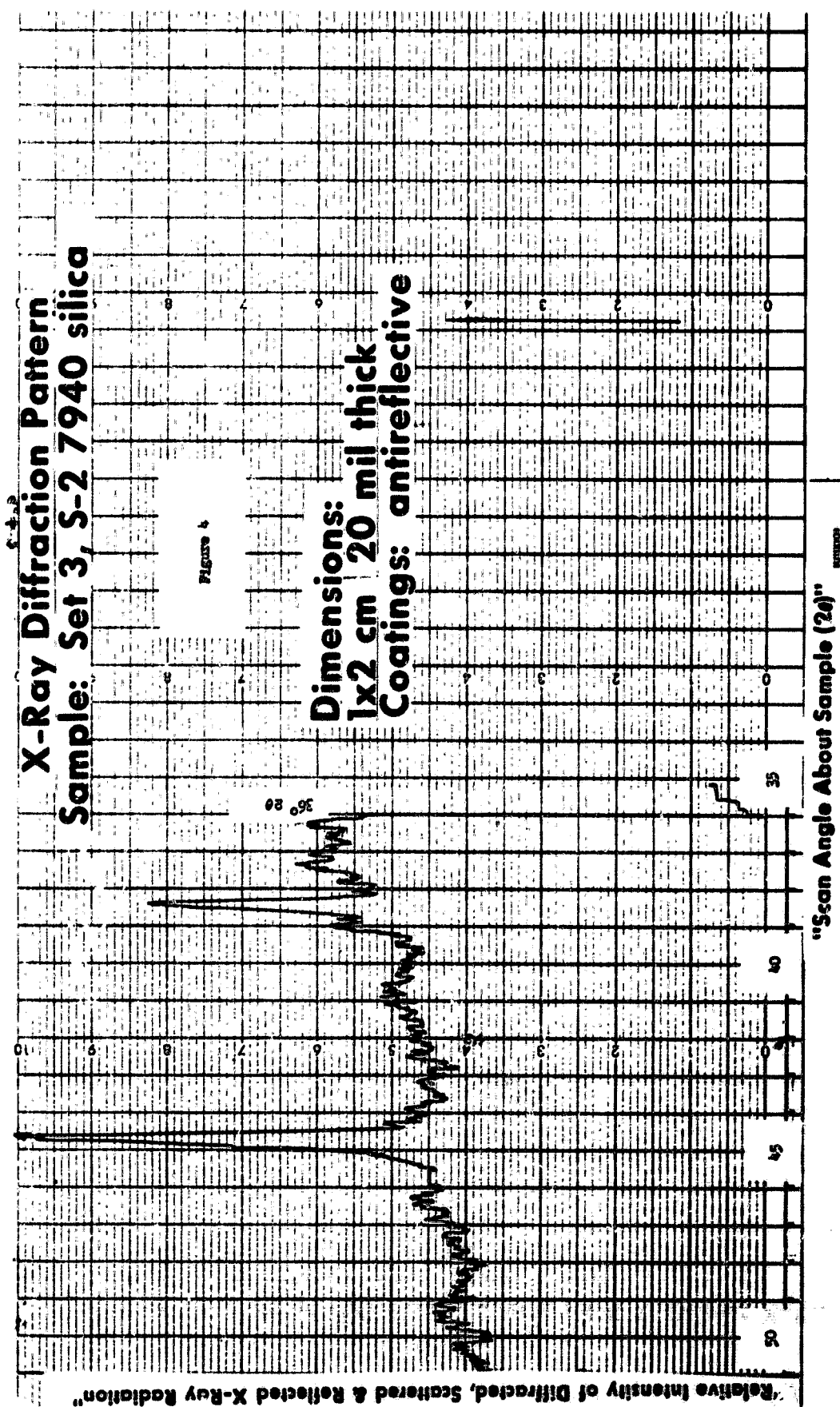
Figure 2

"Relative Intensity of Diffracted, Scattered & Reflected X-Ray Radiation"

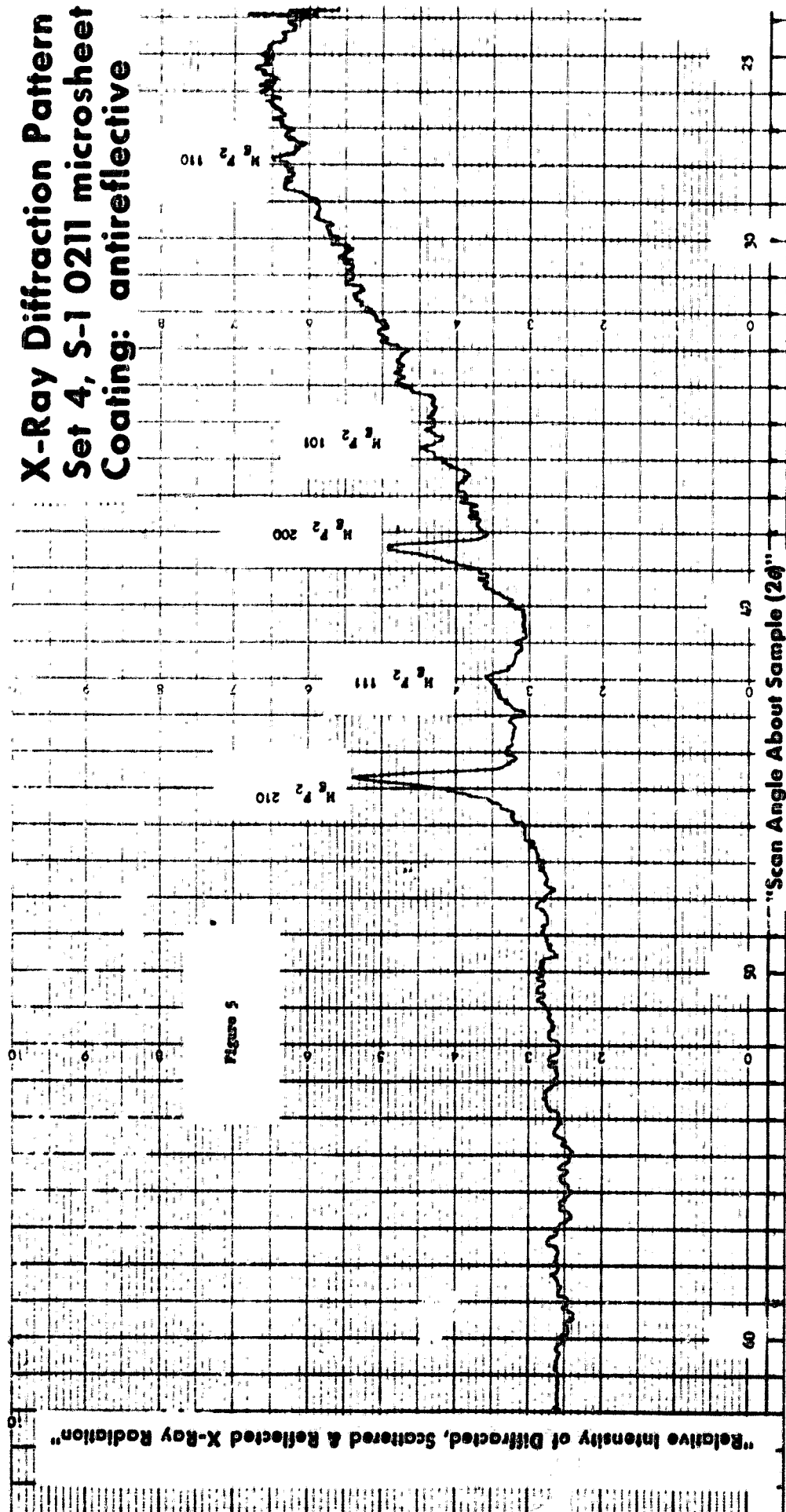
"Scan Angle About Sample (2 θ)"

**X-Ray Diffraction Pattern
Set 2 S-1 7940 silica
Dimensions: 2x2 cm, 3 mil thick
Coating: antireflective
plus ultraviolet filter**



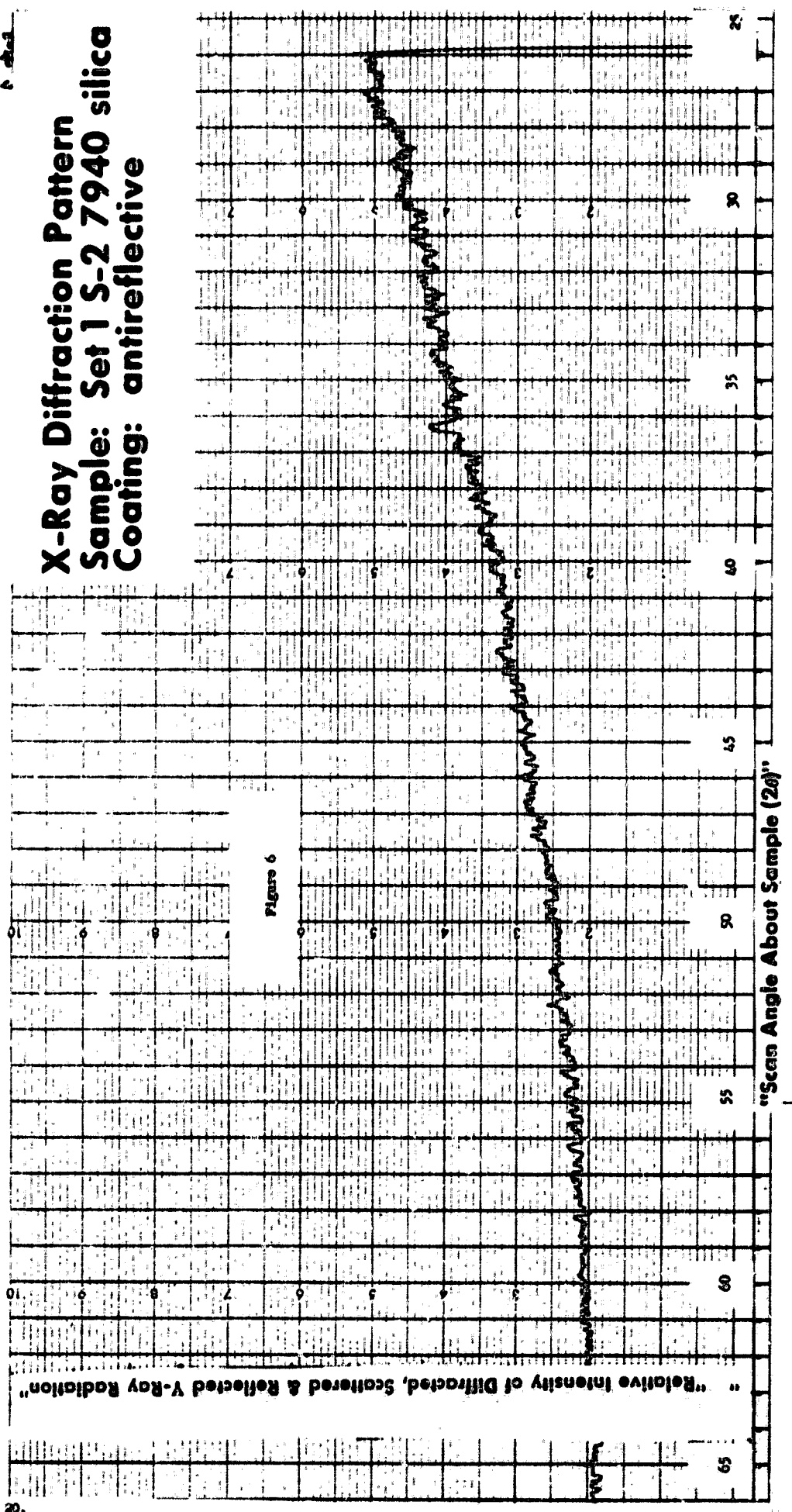


**X-Ray Diffraction Pattern
Set 4, S-1 0211 microsheet
Coating: antireflective**



• ~~4-1~~

X-Ray Diffraction Pattern
Sample: Set 1 S-2 7940 silica
Coating: antireflective



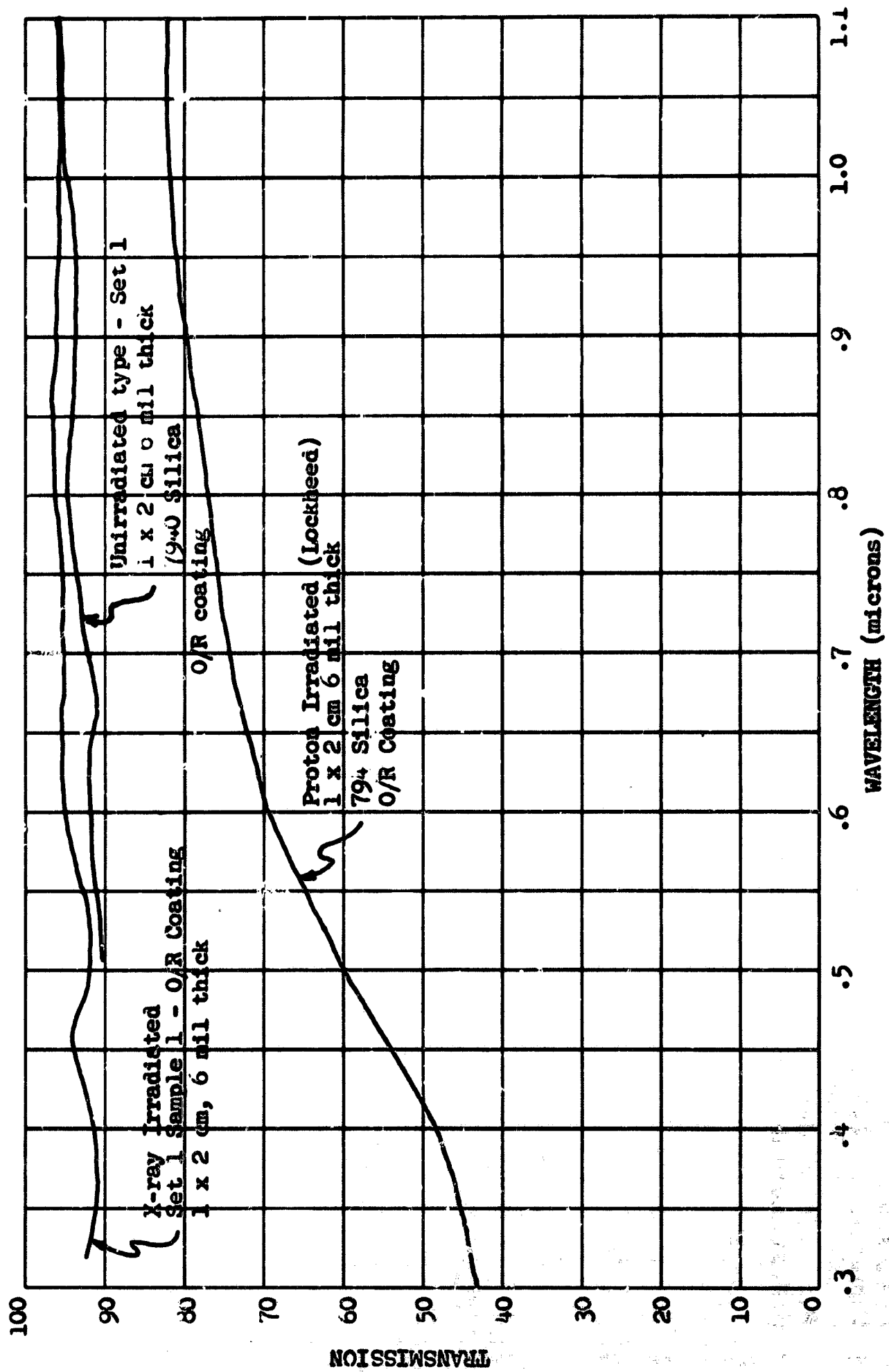


FIGURE 7 - SPECTRA TRANSMISSION OF COVERGLASS

X-Ray Diffractions Pattern

7940 silica Type Set 2

Dimensions: 2×2 cm 3 mil thick

Coating: Antireflective plus ultraviolet filter
Proton irradiated
(Ultraviolet filter facing X radiation)

